

## ORIGINAL ARTICLE

# Coelomycin, a highly substituted 2,6-dioxo-pyrazine fungal metabolite antibacterial agent discovered by *Staphylococcus aureus* fitness test profiling

Michael A Goetz<sup>1</sup>, Chaowei Zhang<sup>1</sup>, Deborah L Zink<sup>1</sup>, Marta Arocho<sup>1</sup>, Francisca Vicente<sup>2,3</sup>, Gerald F Bills<sup>2,3</sup>, Jon Polishook<sup>1</sup>, Karen Dorso<sup>1</sup>, Russell Onishi<sup>1</sup>, Charles Gill<sup>1</sup>, Emily Hickey<sup>1</sup>, Suzy Lee<sup>1</sup>, Richard Ball<sup>1</sup>, Stephen Skwish<sup>1</sup>, Robert GK Donald<sup>1</sup>, John W Phillips<sup>1</sup> and Sheo B Singh<sup>1</sup>

**Bacterial resistance to antibiotics, particularly to multiple antibiotics, is becoming a cause for significant concern. The only really viable course of action to counter this is to discover new antibiotics with novel modes of action. We have recently implemented a new antisense-based chemical genetic screening technology to accomplish this goal. The discovery and antibacterial activity of coelomycin, a fully substituted 2,6-dioxo pyrazine, illustrates the application of the *Staphylococcus aureus* fitness test strategy to natural products discovery.**

*The Journal of Antibiotics* (2010) **63**, 512–518; doi:10.1038/ja.2010.86; published online 28 July 2010

**Keywords:** antibacterial; coelomycin; fitness test; fungal metabolite; pyrazine; *staphylococcus aureus*; target array

## INTRODUCTION

Antibiotic-resistant bacterial strains continue to increase in frequency and pose a serious threat to human lives.<sup>1</sup> Infections by methicillin-resistant *Staphylococcus aureus* alone are responsible for approximately 18 000 deaths per year in the United States.<sup>1</sup> Most of the treatment options available today to treat bacterial infections are the result of incremental improvements to antibiotic lead structures discovered during the 'Golden Age' of antibiotic discovery.<sup>2</sup> Unfortunately, further improvements to those structural leads are proving to be more and more difficult, leading to diminishing return on investment. Obviously, this problem could be alleviated by discovery of new lead classes of antibacterial agents with either known or novel modes of action that could be developed as effective treatment options against drug-resistant bacteria. Most of the antibacterial leads are of natural product origin and natural products remain prolific sources of new antibacterial leads. One of the biggest challenges in natural products discovery remains the rediscovery of known compounds. To improve the probability of success for the discovery of novel natural products, new screening technologies and new sources of natural products are needed. We have tried to address both of these problems. First, we have introduced a target-based whole-cell screening approach that uses inducible antisense to downregulate the expression of individual essential gene targets in *S. aureus*, thereby sensitizing the cells to inhibitors of those targets and enriching the pool of screening hits for inhibitors specific to those targets or pathways at the crude

extract stage.<sup>3</sup> Second, we have expanded our efforts to isolate microorganisms from different geographical regions and habitats (including marine microbes) in combination with improved high-throughput fermentation methods.<sup>4</sup> The combination of these two approaches resulted in the discovery of a large number of natural products using either an *rpsD*-sensitized antisense strain<sup>5–10</sup> or *fabH/fabF* antisense-sensitized strains, including discovery of the *FabF* inhibitors platensimycin and platencin.<sup>11–17</sup>

Recently, we have extended the antisense-based screening approach by constructing a *S. aureus* genome-wide fitness test assay and validated its use by mechanistically profiling a diverse set of 59 antibacterial compounds<sup>18</sup> and by the discovery of a new class of cell wall inhibitors.<sup>19</sup> Included in the *S. aureus* fitness test assay are 245 inducible antisense RNA strains engineered for reduced expression of genes essential for cell growth. Reduced expression of target genes leads to differential growth sensitivity of cells to compounds that inhibit either the targeted gene product or related functions. When combined into pools and grown together for approximately 20 population doublings in the presence of test compounds, these differences in growth lead to specific antisense strains, either being depleted or enriched in the treated population. Using multiplex PCR, capillary electrophoresis and gene fragment analysis to compare the abundances of the strains at the end of the experiment with mock-treated controls generates characteristic antisense-induced strain sensitivity (AISS) profiles that are indicative of the whole-cell

<sup>1</sup>Merck Research Laboratories, Rahway, NJ, USA and <sup>2</sup>CIBE, Merck Sharp & Dohme de Espana, S. A. Josefa Valcárcel, Madrid, Spain

<sup>3</sup>Current address: Fundación Medina, Parque Tecnológico de Ciencias de la Salud, Armilla, Granada, Spain.

Correspondence: Dr SB Singh, RY33-612, Merck Research Laboratories, 126 East Lincoln Avenue, Rahway, NJ 07065, USA.

E-mail: sheo\_singh@merck.com

Dedicated to Professor Arnold Demain, Drew University, for his seminal and pioneering contributions to Fermentation Technology.

Received 22 March 2010; revised 29 April 2010; accepted 16 June 2010; published online 28 July 2010

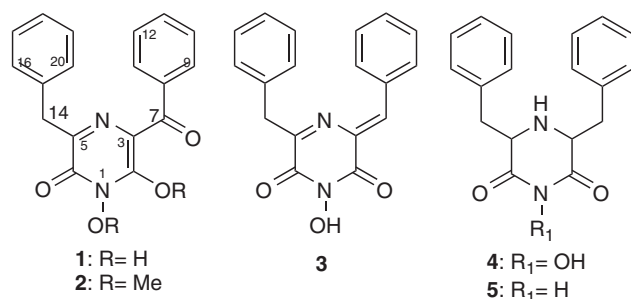


**Figure 1** Chemical structures of coelomycin (1) and its derivatives.

mechanism of action of the compounds. Compound mechanism of action can either be inferred directly from the AISS profile or by comparison with a database of AISS profiles of known inhibitors.<sup>18</sup> Both these phenomena are very useful for the discovery of new compounds by providing not only preliminary mechanistic information but also comparative information that is of great use in dereplicating natural products. Similar to the recent discoveries of parnafungin<sup>20,21</sup> and other novel natural products<sup>22,23</sup> using a *Candida albicans* fitness test assay designed for antifungal discovery,<sup>24</sup> AISS profiling can be used in antibacterial discovery to prioritize extracts for natural products chemistry based on whether their activities are likely working through either known or novel mechanisms of action. Those compounds showing a novel AISS profile and likely containing chemical inhibitors not observed before in the assay can be assigned to isolation chemistry. Those showing a known AISS profile can be further analyzed with HRLCMS and other analytical techniques to either confirm or rule out the presence of known inhibitors before any isolation chemistry steps are undertaken.

Through systematic screening a large number of crude natural product extracts in the *S. aureus* fitness test and comparison of their AISS profiles to those of known inhibitors, we identified an extract from an unidentified Coelomycete fungal strain that produced a unique AISS profile. Bioassay-guided isolation of the extract using a *S. aureus* EP167 strain growth assay led to the isolation of pyrazine (1), named herein coelomycin (Figure 1), which accounted for the AISS profile. The isolation, structure elucidation and details of biological activity including *in vivo* activity of this compound are described.

## RESULTS AND DISCUSSION

As the bacterial target array is not a high-throughput assay, extracts were submitted for primary screening using standard wild-type bacterial strains such as *S. aureus*. Extracts that passed requisite antibacterial activity were selected for AISS profiling analysis. After this triaging process, one of the extracts from an unidentified coelomycete belonging to the Dothideales, isolated from leaf litter of *Juniperus phoenicea* in salt marshes from Roquetas de Mar, Almeria, Spain, produced a distinct AISS profile (Figure 2) with significant depletions of antisense strains for genes involved in cell wall (*mraY*, *murG*, *uppS* and *pbpA*) and fatty acid biosynthesis (*fabI* and *hmrB*). In addition, strong depletions were also observed for the *map*-antisense strain (methionine aminopeptidase–protein synthesis) and to a lesser extent the *thyA*-antisense strain (thymidylate synthase–DNA synthesis). Although this profile contains some strain sensitivities shared with known cell wall or fatty acid synthase inhibitors, the combination of strain depletions is unique to this extract and the AISS profile did not correlate significantly with any AISS profiles for either known inhibitors or undescribed compounds or extracts in our profile database when analyzed using two-dimensional cluster analysis

(data not shown). As this was a unique profile and standard HRLCMS analysis also did not reveal the presence of any obvious antibiotics (data not shown) that could account for any or all of the aspects of the AISS profile, this extract was selected for further studies.

The culture was grown on a glycerol-based liquid medium for 21 days and extracted with equal volume of acetone. Removal of acetone followed by extraction with methyl ethyl ketone, concentration and trituration with methanol provided a semicrystalline solid that was purified by reversed-phase HPLC to afford 47 mg l<sup>-1</sup> of compound 1 as a yellow amorphous powder.

High-resolution electrospray ionization Fourier transformation mass spectrometry analysis of compound 1 provided a molecular formula of C<sub>18</sub>H<sub>14</sub>N<sub>2</sub>O<sub>4</sub> (*m/z* 322.0956) indicating the presence of 13° of unsaturation. The <sup>13</sup>C NMR spectrum in CD<sub>2</sub>Cl<sub>2</sub> (Table 1) showed only 14 carbon signals with four overlapping aromatic carbon signals. The <sup>1</sup>H NMR spectrum showed the presence of 10 aromatic protons from δ<sub>H</sub> 7.30 to δ<sub>H</sub> 8.13, COSY correlations among these protons and the presence of the four overlapping carbon signals, suggesting two monosubstituted phenyl rings. The presence of a downfield shifted methylene singlet (δ<sub>H</sub> 4.12, δ<sub>C</sub> 39.3) and its heteronuclear multibond connectivity (HMBC) correlation with aromatic carbons at δ<sub>C</sub> 130.1 and 136.9 showed that one of the phenyl groups was present as a benzyl unit. One of the protons resonating at δ<sub>H</sub> 8.13 showed HMBC correlation with a carbonyl resonating at δ<sub>C</sub> 180.4, suggesting that the second phenyl group was a benzoyl unit. Together, the benzyl and benzoyl units account for 14 of 18 carbons. The four unassigned carbons resonated at δ<sub>C</sub> 161.8, 115.6, 147.4 and 152.8. Taking into consideration the presence of two nitrogens and three additional oxygens indicated that this molecule is a diketopiperazine with extended conjugation similar to flutimide.<sup>25–27</sup> This assumption was supported by the IR and UV spectra. The HMBC correlations of the methylene protons with δ<sub>C</sub> 147.4 established the substitution of benzyl group at C-5. The NMR data did not allow to differentiate between a 2,6-diketopiperazine and a 2,5-diketopiperazine and thus could not define the position of the benzoyl group (C-3 or C-2). It was clear from the presence of a OH group at δ<sub>H</sub> 15.8 that the keto group was enolized and formed a strong six-centered H-bond with the benzoyl ketone. Methylation of compound 1 with diazomethane produced dimethyl ether 2. The methoxy group (δ<sub>H</sub> 4.10, δ<sub>C</sub> 64.7) showed HMBC correlation with δ<sub>C</sub> 154.0 and the benzoyl keto group showed HMBC correlation with H-9/13 δ<sub>H</sub> 7.83, suggesting that the benzoyl keto was not enolized. However, methylation still did not allow for distinction of 2,6- versus 2,5-diketo substitution.

LiBH<sub>4</sub> reduction of compound 1 produced deoxy compound 3 (*m/z* 306.1007; C<sub>18</sub>H<sub>14</sub>N<sub>2</sub>O<sub>3</sub>) that showed <sup>1</sup>H and <sup>13</sup>C NMR spectra identical to sclerominol.<sup>28</sup> Hydrogenation of compound 1 with Pd/C afforded tetrahydro deoxy compound 4 (C<sub>18</sub>H<sub>18</sub>N<sub>2</sub>O<sub>3</sub>) and tetrahydro dideoxy compound 5 (C<sub>18</sub>H<sub>18</sub>N<sub>2</sub>O<sub>2</sub>). <sup>13</sup>C NMR spectrum (Table 2) of compound 4 showed only seven carbon resonances indicating C2 symmetry. The methine protons δ<sub>H</sub> 3.70 (δ<sub>C</sub> 60.2) of compound 4 showed HMBC correlations with the methylene carbon (δ<sub>C</sub> 36.8), aromatic carbon (δ<sub>C</sub> 137.7) and carbonyl (δ<sub>C</sub> 169.5) and most importantly with its carbon confirming the 2,6-diketopiperazine structure 4. The <sup>13</sup>C NMR spectrum of compound 5 was similar to the spectrum of 4 with the exception of 4 p.p.m. downfield shifted carbonyl resonance (Table 2) due to loss of the N-oxy group. On the basis of the structure of 4 and 5, benzoyl group was placed at C-3 and structure 1 was assigned to compound 1. This could be confirmed in the following way: compound 1 was crystallized from aqueous methanol for X-ray crystallographic studies that showed enolization of benzoyl ketone (Figure 3), whereas in aprotic solvent the C-2 keto

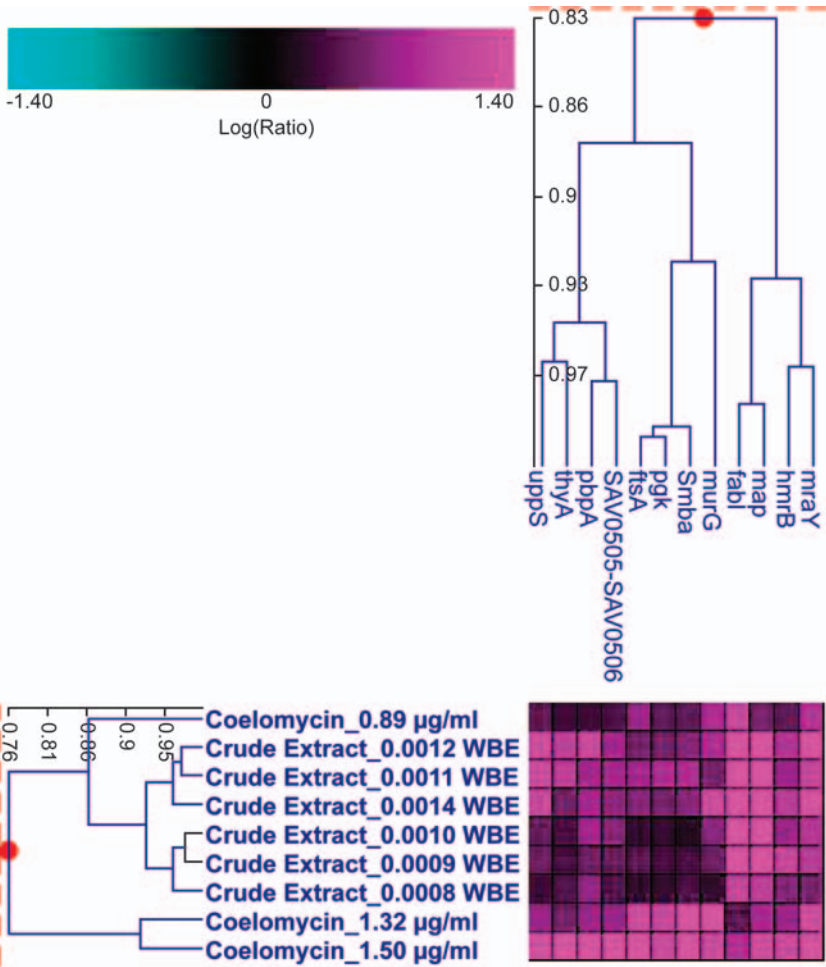


**Figure 2** *S. aureus* fitness test analysis of crude extract and coelomycin (**1**) samples. This two-dimensional cluster of antisense-induced strain sensitivity (AISS) profiles shows the similarity between the profiles of the crude extract and pure compound. Strain depletions are represented in magenta and strain resistances in cyan. The extract or compound name is followed by the treatment concentration. The 12 antisense strains shown in the cluster are those with significant hypersensitivity to the treatments. The thresholds for including strains in the analysis are >5-fold depletion, *P*-value ≤0.01 in ≥3 experiments. The data from a dose titration at sub-MIC concentrations are shown.

**Table 1** <sup>1</sup>H (500 MHz) and <sup>13</sup>C (125 MHz) NMR assignment of compounds **1–3** in CD<sub>2</sub>Cl<sub>2</sub>

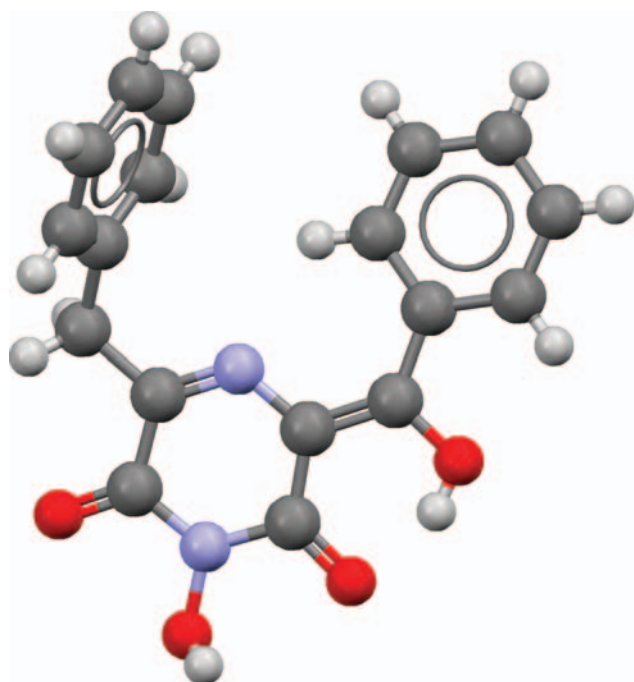
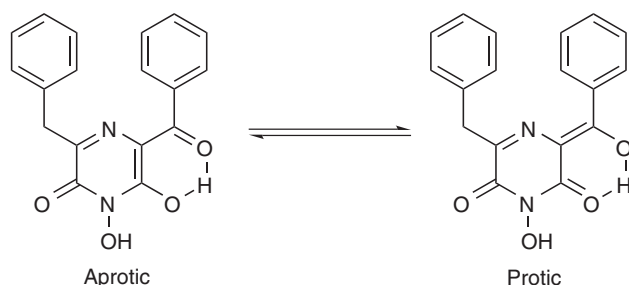
No.	<b>1</b>			<b>2</b>			<b>3</b>		
	$\delta_H$ (mult, J in Hz)	$\delta_C$	HMBC (H→C)	$\delta_H$ (mult, J in Hz)	$\delta_C$	HMBC (H→C)	$\delta_H$ (mult, J in Hz)	$\delta_C$	HMBC (H→C)
2		161.8			154.0			159.4	
3		115.6			120.4			131.9	
5		147.4			151.9			152.2	
6		152.8			152.7			157.0	
7		180.4			190.0		7.84 (s)	144.6	C-2, 9/13
8		131.9			137.8			133.6	
9, 13	8.13 (d, 7.6 Hz)	132.1	C-7, 11, 13/9	7.83 (brd, 8.2 Hz)	130.7	C-7, 11, 13/9	7.97 (brd, 7.8 Hz)	134.9	C-7, 11, 13/9
10, 12	7.40 (m)	128.5	C-8, 11, 10/12	7.44 (t, 7.7 Hz)	128.3	C-10/12, 8	7.34 (m)	129.2	C-8
11	7.57 (t, 7.4 Hz)	133.7	C-9/13, 10/12	7.57 (tt, 7.5 Hz)	132.8	C-9/13	7.46 (t, 7.2 Hz)	132.8	C-9/13
14	4.12 (s)	39.3	C-5, 15, 16/20	4.06 (s)	39.6	C-16/20, 15, 5	4.22 (s)	40.0	C-5, 6, 15, 16/20
15		136.9			137.6			135.9	
16, 20	7.31 (m)	130.1	C-14, 18	7.32 (m)	129.8	C-18, 14, 20/16	7.35 (m)	130.4	C-14, 18
17, 19	7.34 (m)	128.8	C-15, 19/17	7.28 (m)	128.7	C-15, 19/17	7.38 (m)	129.0	C-15
18	7.30 (m)	127.1	C-16/20	7.22 (tt, 7.2 Hz)	126.9	C-16/20	7.34 (m)	127.3	
OH	15.80 (brs)								
N-OMe				4.08 (s)	65.5				
OMe				4.10 (s)	64.7	C-2			

Abbreviation: HMBC, heteronuclear multibond connectivity.

**Table 2**  $^1\text{H}$  (500 MHz) and  $^{13}\text{C}$  (125 MHz) NMR assignment of compounds **4** and **5** in  $\text{CD}_2\text{Cl}_2$ 

No.	<b>4</b>			<b>5</b>		
	$\delta_{\text{H}}$ (mult, J in Hz)	$\delta_{\text{C}}$	HMBC (H $\rightarrow$ C)	$\delta_{\text{H}}$ (mult, J in Hz)	$\delta_{\text{C}}$	HMBC (H $\rightarrow$ C)
2/6		169.5			173.2	
3/5	3.70 (dd, 8.5, 3.9 Hz)	60.2	C-2/6, 8, 5/3, 7	3.55 (dd, 8.6, 3.9 Hz)	60.0	C-2/6, 8, 5/3, 7
7	2.93 (dd, 13.8, 8.5 Hz)	36.8	C-2/6, 8, 9, 3/5	2.85 (dd, 13.9, 8.6 Hz)	36.3	C-2/6, 8, 9, 3/5
	3.36 (dd, 13.8, 3.9 Hz)			3.33 (dd, 13.9, 3.9 Hz)		
8		136.7			136.9	
9	7.14 (m)	129.7	C-9, 11, 7	7.12 (m)	129.8	C-9, 11, 7
10	7.23 (m)	129.0	C-8, 10	7.20 (m)	129.2	C-8, 10
11	7.20 (m)	127.3	C-9	7.17 (m)	127.4	C-9

Abbreviation: HMBC, heteronuclear multibond connectivity.

**Figure 3** X-ray crystal structure of coelomycin (**1**).**Figure 4** Tautomeric forms of compound **1** in protic and aprotic solvents.

group is enolized. Both enolizations lead to six-centered hydrogen bond (Figure 4). The protic tautomeric form is likely the form that predominates in aqueous systems and is perhaps the biologically active form.

While our studies were in progress, Chinworrungsee *et al.*<sup>29</sup> reported the isolation of compound **1** from *Menisporopsis theobromae* BCC3975. They reported antimalarial ( $\text{IC}_{50}$  28.8  $\mu\text{M}$ ) and

antimycobacterial ( $\text{MIC}$  310.5  $\mu\text{g ml}^{-1}$ ) activities. These researchers did not name the compound, and hence we named it coelomycin.

### Biological activity

Coelomycin (**1**) was first evaluated in the *S. aureus* genome-wide fitness test to establish the AISS profile for the purified compound **1**. Comparison of the AISS profile for coelomycin (**1**) with that of the acetone extract revealed a similar profile with shared depletions in antisense strains for cell wall, fatty acid, protein and DNA synthesis (Figure 2). This step of the analysis confirms the isolation of the sought-after compound that was responsible for the profile in the extract and further establishes that this multipathway profile is the result of the biological actions of a single antibacterial agent.

Coelomycin was further evaluated for its antibacterial activities against a panel of clinically relevant Gram-positive and Gram-negative bacterial strains and the data are summarized in Table 3. This compound was essentially inactive when tested in standard CLSI (Clinical and Laboratory Standards Institute) conditions in CAMHB (cation-adjusted Mueller Hinton broth) medium. However, it showed good activity when bacteria were grown in other media. For example, it inhibited growth of *S. aureus* Smith with an MIC value(s) of 4  $\mu\text{g ml}^{-1}$  in iso-sensitest medium and 0.25–0.5  $\mu\text{g ml}^{-1}$  in nutrient broth medium supplemented with 10% NaCl. It showed similar activity against *Streptococcus pneumoniae* (MIC 4  $\mu\text{g ml}^{-1}$ ) in iso-sensitest medium. It was also active against *Haemophilus influenzae* (MIC 8  $\mu\text{g ml}^{-1}$ ) in HTM medium. It did not show any activity against wild-type *Escherichia coli* but was effective against *E. coli* strain (MIC 0.5–2  $\mu\text{g ml}^{-1}$ ) harboring mutations in envelope proteins and *tolC* pump, suggesting that the compound either does not enter the cells or is pumped out in the wild-type bacteria. To probe the effect of cations, this compound was further tested in a few growth media in the presence of  $\text{Ca}^{+2}$  or  $\text{Mg}^{+2}$  and the data are summarized in Table 4. The presence of excess bivalent cations has a detrimental effect on the activity of this compound in LB (Lysogeny broth) medium but not in nutrient broth medium. In a macromolecular synthesis inhibition assay, compound **1** inhibited all five (DNA, RNA, protein, peptidoglycan and phospholipid) with a modest four-fold selectivity for cell wall synthesis (Figure 5). These data are consistent with the AISS profile data that showed depletion of a number of cell wall-associated antisense strains along with depletions in antisense strains associated with several other biological processes (Figure 2). Compounds **2**–**5** were significantly less active and did not show any antibacterial activity at 64  $\mu\text{g ml}^{-1}$  against *S. aureus* EP167 strain.

Coelomycin did not show efficacy in a murine disseminated target organ assay against *S. aureus*. The compound was dosed twice daily by



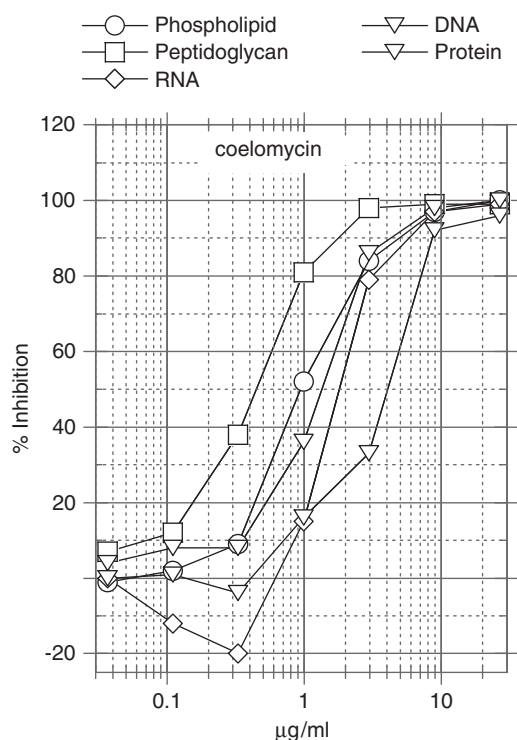
**Table 3** *In vitro* antibacterial activity of coelomycin (1) (MIC in  $\mu\text{g mL}^{-1}$ )

Organism	Strain no.	CAMHB	NB+10% NaCl	Iso-sensitest	HTM
<i>S. aureus</i> (MSSA)	MB2865	> 16	0.5	4	NT
<i>S. aureus</i>	EP167	> 16	0.25	4	NT
<i>Streptococcus pneumoniae</i> (penicillin <sup>S</sup> )	CL2883	> 16 <sup>a</sup>	NT	4	NT
<i>Haemophilus influenzae</i>	MB4572	> 16	NT	NT	8
<i>Escherichia coli</i>	MB2884	> 16	> 8	> 8	NT
<i>E. coli</i> envA, tolC	MB5746	> 16	0.5	2	NT
<i>Candida albicans</i>	MY1055	> 16 <sup>b</sup>	NT	NT	NT

Abbreviations: CAMHB, cation-adjusted Mueller Hinton broth; MSSA, methicillin-sensitive *Staphylococcus aureus*; NB, nutrient broth.<sup>a</sup>Medium: CAMHB +2.5% lysed horse blood.<sup>b</sup>In YPD (richest) and Sab-Dex media.**Table 4** Effect of media on MIC ( $\mu\text{g mL}^{-1}$ ) of coelomycin (1)

Media	<i>S. aureus</i> EP167
NB	0.2–0.4
NB+0.2% YE	0.8
NB+0.2% YE+1% NaCl	0.8–1.6
LB	0.8–3.2
CAMHB	$\geq 25$
BHI	6.25
NB+Mg <sup>2+</sup> /Ca <sup>2+</sup> <sub>a</sub>	0.4
LB+Mg <sup>2+</sup> /Ca <sup>2+</sup> <sub>a</sub>	25

Abbreviations: BHI, brain heart infusion broth; CAMHB, cation-adjusted Mueller Hinton broth; LB, Lysogeny broth; NB, nutrient broth; YE, yeast extract.

<sup>a</sup>Both Ca<sup>2+</sup> (25 mg L<sup>-1</sup>) and Mg<sup>2+</sup> (12.5 mg L<sup>-1</sup>) were used as chlorides.**Figure 5** Inhibition of macromolecular synthesis by coelomycin.

subcutaneous route at 50 mg kg<sup>-1</sup> in cremaphor formulation. This lack of efficacy may perhaps be due to poor exposure. At 50 mg kg<sup>-1</sup>, it showed an area under the curve (AUC) of 1.07  $\mu\text{M h mg kg}^{-1}$  with normalized AUC of 0.28  $\mu\text{M h mg kg}^{-1}$ . Unfortunately, the PK was not

linear and the compound produced better exposures at 25 (AUC 1.80  $\mu\text{M h}$ ) and 12.5 (AUC 1.84  $\mu\text{M h}$ ) mg kg<sup>-1</sup>. The compound was not tested at higher doses because of poor solubility and lack of PK linearity. Coelomycin did not show toxicity to a number of mammalian cells (human embryo kidney, Chinese hamster ovary and Hela cells) at 50  $\mu\text{g mL}^{-1}$ .

In summary, in this study we report the application of an antisense-based *S. aureus* fitness test platform to the discovery of new natural product antibiotics. This led to the discovery of coelomycin, (at the time it was a novel compound), a broad-spectrum Gram-positive antibacterial agent. Both AISS profiling and a macromolecular synthesis inhibition assay suggested that coelomycin inhibits bacterial growth by multiple modes of action with a slight preference for peptidoglycan (cell wall) synthesis inhibition. Although the mechanism of action of coelomycin remains to be resolved, this report shows that a unique AISS profile in an acetone extract can lead to the isolation of novel chemical entities. This compound did not show any *in vivo* activity due to poor exposure.

## EXPERIMENTAL PROCEDURE

### General experimental procedures

HP1100 (Agilent, Santa Clara, CA, USA) was used for analytical HPLC. The UV spectra were recorded in MeOH/THF 1:1 on a Perkin-Elmer Lambda 35 Spectrometer (Perkin Elmer, Waltham, MA, USA). IR spectra were recorded on a Perkin-Elmer Spectrum One spectrometer. Electrospray ionization MS data were recorded on an Agilent 1100 mass selective detector with electrospray ionization. High-resolution electrospray ionization Fourier transformation mass spectrometry was acquired on a Thermo Finnigan LTQ-FT (Thermo Fisher Scientific, Waltham, MA, USA) with the standard Ion Max API source (without the sweep cone) and electrospray ionization probe. Three scan events were used. The ion trap was scanned from 150 to 2000, first in negative ion mode and then in positive ion mode. The FT was scanned from 200 to 2000 in the positive ion mode only. In all cases, the SID was set to 18 V to try to reduce multiple ion clusters. Instrument resolution was set to 100 000 at *m/z* 400. No internal calibration was required; the instrument was calibrated once a week and checked daily to assure accuracy. All NMR spectra were recorded using a Varian Unity 500 (<sup>1</sup>H, 500 MHz, <sup>13</sup>C, 125 MHz) spectrometer (Varian, Palo Alto, CA, USA). The residual proton of CD<sub>2</sub>Cl<sub>2</sub> was used as an internal reference ( $\delta_{\text{H}}$  5.32,  $\delta_{\text{C}}$  54.0). The COSY, DEPT, heteronuclear multiple quantum coherence (HMQC) and HMBC spectra were measured using standard Varian pulse sequences.

### Producing organism and fermentation

The producing microfungus, an unidentified coelomycete, was isolated from leaf litter of *Juniperus phoenicea* in the salt marshes of Roquetas de Mar, Almeria, Spain. Sequencing of the ITS1/5.8S/ITS4 region of the ribosomal DNA followed by sequence similarity searches in GenBank indicated that this strain was remotely related to a number of fungi in the Dothideales. Among the most similar internal transcribed spacer sequences retrieved were: *Kabatina juniperi* AF182376.2 (92%), *Kabatina thujae* AF013226 (91%), *Dothidea berberidis* CBS

186.58 (92%) and *Dothidea muelleri* CBS 191.58 (91%). Fermentation of this culture was accomplished by inoculating several agar plugs with mycelia into a seed broth flask (50 ml medium in 250 ml unbaffled flask). The formulation for the seed broth was as follows (g per liter, unless specified): corn steep liquor, 5.0; tomato paste, 40.0; oat flour, 10.0; glucose, 10.0; trace element mix, 10.0 ml l<sup>-1</sup>; and agar, 4.0. The pH was adjusted to 6.8 with NaOH before sterilization. The formulation for the trace element mix consisted of (g per liter): FeSO<sub>4</sub>·7H<sub>2</sub>O, 1.0; MnSO<sub>4</sub>·H<sub>2</sub>O, 1.0; CuCl<sub>2</sub>·2H<sub>2</sub>O, 0.025; CaCl<sub>2</sub>, 0.1; H<sub>3</sub>BO<sub>3</sub>, 0.056; (NH<sub>4</sub>)<sub>6</sub>Mo<sub>7</sub>O<sub>24</sub>·4H<sub>2</sub>O, 0.019; and ZnSO<sub>4</sub>·7H<sub>2</sub>O, 0.2, prepared in 0.6N HCl. The flasks were incubated at 22 °C with 80% relative humidity and shaken on a rotary shaker at 220 r.p.m. After the seed stage flasks have grown for 4–7 days, a 1 ml aliquot was used to inoculate each flask of the production medium (50 ml medium in a 250 ml unbaffled flask). The formulation of production medium consisted of (g per liter): glycerol, 125.0; glucose, 25.0; pectin, 20.0; ardamine pH, 5.0; (NH<sub>4</sub>)<sub>2</sub>SO<sub>4</sub>, 4.0; KH<sub>2</sub>PO<sub>4</sub>, 4.0; and CoCl<sub>2</sub>·6H<sub>2</sub>O, 0.1. The pH was adjusted to 7.0 with NaOH before sterilization. The flasks were incubated at 22 °C with 80% relative humidity on a rotary shaker at 220 r.p.m. for 21 days.

### *S. aureus* fitness test

The *S. aureus* fitness test assay was performed as previously described.<sup>18</sup> In brief, 245 strains each containing a different inducible antisense RNA interference plasmid targeting an essential gene in *S. aureus* RN4220 were pooled into 24 different bins of 6–12 strains each. The bins were then grown each at a different concentration of xylose inducer (ranging from 1.8 to 55 mM) for ~20 population doublings either in the presence of acetone extract or compound being tested or as a 2% DMSO mock treatment control. Strain bin growth was performed in 384-well plates (Costar 3680; Corning Life Sciences, Acton, MA, USA) on a fully automated system using LB media containing chloramphenicol (34 µg ml<sup>-1</sup>) over three cycles of growth ranging from 5 to 7 h each for a total time of ~18 h in a total volume of 50 µl. At the end of the growth period, cells from all 24 bins were pooled for each test treatment or DMSO mock treatment control. Pooled cells were then lysed and subjected to multiplex PCR to amplify specific antisense markers for each strain. Strain-specific markers were subsequently identified and peak areas quantified by DNA fragment analysis using an ABI 3730 genetic analyzer (Applied Biosystems, Carlsbad, CA, USA). Peak areas were then normalized and strain depletion ratios were calculated. Statistical significance was determined as a *P*-value using an error model generated for each individual strain across a discrete set of known standards and unknown test samples selected to represent total coverage of all strains within the array set.

### Extraction and isolation

Acetone (5l) was added to 5l fermentation broth and shaken for 1 h and filtered through celite to remove cells. The extract was concentrated under reduced pressure to remove most of the acetone, and then partitioned into methyl ethyl ketone (2×3l). The organic extract was concentrated under reduced pressure to dryness to yield a solid residue that was triturated with aqueous MeOH to give semicrystalline solid. This was dissolved in DMSO and directly injected on a preparative reversed-phase HPLC column (Zorbax RX C<sub>8</sub>, 21.2×250 mm; Agilent, Santa Clara, CA, USA) eluting with a 90-min gradient of 10–100% aqueous CH<sub>3</sub>CN + 0.1% TFA at a flow rate of 10 ml min<sup>-1</sup>. Lyophilization of the major peak from a number of runs yielded 377 mg of compound **1** (47.1 mg l<sup>-1</sup>) as an amorphous yellow powder. Coelomycin (**1**): UV (CHCl<sub>3</sub>) λ<sub>max</sub> 265 (ε 13 298) 375 (ε 21 091) nm; IR (ZnSe) ν<sub>max</sub> 3437, 2926, 1639, 1674, 1585, 1519, 1489, 1436, 1356, 1220, 1073, 1035, 960 cm<sup>-1</sup>; <sup>1</sup>H and <sup>13</sup>C NMR data, see Table 1; and HRESI-FTMS *m/z* 322.0956 (calcd for C<sub>18</sub>H<sub>14</sub>N<sub>2</sub>O<sub>4</sub>: 322.0954).

### Methylation of coelomycin (**1**)

An aliquot of 20 mg (0.062 mmol) was added to a mixture of 4 ml anhydrous CH<sub>2</sub>Cl<sub>2</sub> and 1 ml anhydrous ether. To this stirred solution was added 2.5 ml (0.4 M) ethereal solution of freshly prepared diazomethane. After 90 min, reaction was stopped by addition of AcOH. Solution was concentrated under a stream of nitrogen and the residue was redissolved in 500 µl MeOH and chromatographed by preparative reversed-phase HPLC using a Zorbax RX C<sub>8</sub> (21.2×250 mm) column eluting with a 45-min gradient of 20–40%, followed by a 15-min gradient of 40–95%, and then holding at 95% aqueous CH<sub>3</sub>CN

containing 0.1% TFA at a flow rate of 10 ml min<sup>-1</sup>. Lyophilization of fractions eluting at 60 min afforded 4.2 mg of compound **2** as a light-yellow amorphous powder. (**2**): UV (CH<sub>3</sub>OH/THF 1:1) λ<sub>max</sub> 209 (ε 13 210) 251 (ε 6436) 306 (ε 8728) nm; IR (ZnSe) ν<sub>max</sub> 2943, 1682, 1651, 1598, 1450, 1380, 1324, 1181, 982, 947 cm<sup>-1</sup>; <sup>1</sup>H and <sup>13</sup>C NMR data, see Table 1; and HRESI-FTMS *m/z* 350.1263 (calcd for C<sub>20</sub>H<sub>18</sub>N<sub>2</sub>O<sub>4</sub>: 350.1267).

### Synthesis of 1-hydroxy-3-benzylene-5-benzyl-pyrazine-2,6-dione (**3**)

A 5 mg (0.015 mmol) aliquot of **1** was added to 0.5 ml lithium borohydride solution in THF and stirred for 2 h. Reaction was quenched with 2.5 ml 5% acetic acid in MeOH and the product was chromatographed by gel filtration on Sephadex LH-20 (GE Healthcare, Uppsala, Sweden; 10 ml column, gravity elution, eluted with 100% MeOH, 2 ml per fraction). Fractions 4 and 5 were combined and concentrated to dryness. The residue was redissolved in 1.5 ml MeOH, diluted with 8 ml H<sub>2</sub>O and chromatographed on Amberchrome resin (Rohm and Haas, Philadelphia, PA, USA; 5 ml column, washed with 10% MeOH and eluted with 100% MeOH). The fractions eluting with 100% MeOH were concentrated to dryness and were further fractionated by semi-prep HPLC using Zorbax C<sub>8</sub> (9.4×250 mm) column eluting with a 45-min gradient of 25–35%, and a 15-min gradient of 35–95% aqueous CH<sub>3</sub>CN containing 0.1% TFA at a flow rate of 5 ml min<sup>-1</sup>. Lyophilization of fractions eluting at 51 min afforded 1.2 mg of compound **3** as light-yellow amorphous powder. (**3**): UV (CH<sub>3</sub>OH/THF 1:1) λ<sub>max</sub> 242 (ε 6104) 351 (ε 6890) nm; IR (ZnSe) ν<sub>max</sub> 3248, 2926, 1674, 1615, 1580, 1563, 1495, 1454, 1365, 1252, 1179, 1072, 1031, 967 cm<sup>-1</sup>; <sup>1</sup>H and <sup>13</sup>C NMR data, see Table 1; and HRESI-FTMS *m/z* 306.1007 (calcd for C<sub>18</sub>H<sub>14</sub>N<sub>2</sub>O<sub>3</sub>: 306.0999).

### Hydrogenation of coelomycin

A solution of 5 mg (0.015 mmol) of **1** in 0.5 ml THF was treated with 5% Pd/C and was saturated with hydrogen filled in a balloon. Reaction was stirred for days and catalyst was removed by filtration through a Whatman 0.2 µm filter (GE Healthcare, Piscataway, NJ, USA). The solvent was removed under a stream of nitrogen and the residue was dissolved in MeOH and fractionated by semi-prep HPLC using Zorbax C<sub>8</sub> (9.4×250 mm) column eluting with a 45-min gradient of 25–40% aqueous CH<sub>3</sub>CN at a flow rate of 5 ml min<sup>-1</sup>. Lyophilization of fractions eluting at 31 min and 39 min afforded 1.4 mg of compound **4** and 0.4 mg of compound **5** as colorless amorphous powders, respectively. (**4**): UV (CH<sub>3</sub>OH/THF 1:1) λ<sub>max</sub> 205 (ε 55 800) nm; IR (ZnSe) ν<sub>max</sub> 3274, 1699, 1684, 1559, 1496, 1436, 1256, 1203, 1135, 1073, 973 cm<sup>-1</sup>; <sup>1</sup>H and <sup>13</sup>C NMR data, see Table 2; and HRESI-FTMS *m/z* 310.1317 (calcd for C<sub>18</sub>H<sub>18</sub>N<sub>2</sub>O<sub>3</sub>: 310.1312). (**5**): UV (CH<sub>3</sub>OH/THF 1:1) λ<sub>max</sub> 201 (ε 18 404) nm; IR (ZnSe) ν<sub>max</sub> 2929, 1699, 1651, 1559, 1497, 1455, 1436, 1206, 973 cm<sup>-1</sup>; <sup>1</sup>H and <sup>13</sup>C NMR data, see Table 2; and HRESI-FTMS *m/z* 294.1367 (calcd for C<sub>18</sub>H<sub>14</sub>N<sub>2</sub>O<sub>2</sub>: 294.1363).

### X-ray of coelomycin

Compound (**1**) C<sub>18</sub>H<sub>14</sub>N<sub>2</sub>O<sub>4</sub>, *Mr*=322.310, orthorhombic, *P*212121, *a*=4.8388(2), *b*=16.9567(7), *c*=17.7886(8) Å, *V*=1459.56(11) Å<sup>3</sup>, *Z*=4, *D<sub>x</sub>*=1.467 g cm<sup>-3</sup>, monochromatized radiation λ(Mo)=0.71073 Å, μ=0.11 mm<sup>-1</sup>, *F*(000)=672, *T*=100 K. Data were collected on a Bruker CCD diffractometer (Bruker, Madison, WI, USA) to a θ limit of 32.07° that yielded 17 858 reflections. There are 5096 unique reflections with 4003 observed at the 2σ level. The structure was solved by direct methods (SHELXS-97; Sheldrick<sup>30</sup>) and refined using full-matrix least-squares on *F*<sup>2</sup> (SHELXL-97; Sheldrick<sup>31</sup>). The final model was refined using 219 parameters and all 5096 data. All non-hydrogen atoms were refined with anisotropic thermal displacements. The final agreement statistics were: *R*=0.046 (based on 4003 reflections with *I*>2σ(*I*)), *wR*=0.087, *S*=1.02 with (Δ/σ)<sub>max</sub>=0.01. The maximum peak height in a final difference Fourier map was 0.308 eÅ<sup>-3</sup> and this peak was without chemical significance. CCDC (Cambridge Crystallographic Data Centre) nnnnnn contains the supplementary crystallographic data for this paper. These data can be obtained free of charge from the CCDC through [www.ccdc.cam.ac.uk/data\\_request/cif](http://www.ccdc.cam.ac.uk/data_request/cif).

### MIC

The MIC against each of the strains was determined as previously described.<sup>32</sup> The medium with a two-fold serial dilution of compounds in BHI (brain heart infusion) broth was inoculated with 10<sup>5</sup> CFU per ml, and was incubated at

37 °C for 20 h. MIC is defined as the lowest concentration of antibiotic that inhibits visible growth.

### Inhibition of macromolecular synthesis

The assay was performed as previously described for whole-cell labeling assay.<sup>11,33</sup>

### In vivo efficacy

Details of the method have been previously described.<sup>34</sup>

- 1 Klevens, R. M. *et al.* Invasive methicillin-resistant *Staphylococcus aureus* infections in the United States. *J. Am. Med. Assoc.* **298**, 1763–1771 (2007).
- 2 Singh, S. B. & Barrett, J. F. Empirical antibacterial drug discovery-foundation in natural products. *Biochem. Pharmacol.* **71**, 1006–1015 (2006).
- 3 Singh, S. B., Phillips, J. W. & Wang, J. Highly sensitive target based whole cell antibacterial discovery strategy by antisense RNA silencing. *Curr. Opin. Drug Disc. Dev.* **10**, 160–166 (2007).
- 4 Bills, G. F. *et al.* Enhancement of antibiotic and secondary metabolite detection from filamentous fungi by growth on nutritional arrays. *J. Appl. Microbiol.* **104**, 1644–1658 (2008).
- 5 Singh, S. B. *et al.* Discovery of lucensimycins A and B from *Streptomyces lucensis* MA7349 using an antisense strategy. *Org. Lett.* **8**, 5449–5452 (2006).
- 6 Ondeyka, J. G. *et al.* Coniothyron, a chlorocyclopentadienylbenzopyrone as a bacterial protein synthesis inhibitor discovered by antisense technology. *J. Nat. Prod.* **70**, 668–670 (2007).
- 7 Singh, S. B., Zink, D. L., Herath, K. B., Salazar, O. & Genilloud, O. Discovery and antibacterial activity of lucensimycin C from *Streptomyces lucensis*. *Tetrahedron Lett.* **49**, 2616–2619 (2008).
- 8 Singh, S. B. *et al.* Isolation, structure, and antibacterial activities of lucensimycins D-G, discovered from *Streptomyces lucensis* MA7349 using an antisense strategy (perpendicular). *J. Nat. Prod.* **72**, 345–352 (2008).
- 9 Zhang, C. *et al.* Discovery of okilactomycin and congeners from *Streptomyces scabrisporus* by antisense differential sensitivity assay targeting ribosomal protein s4. *J. Antibiot. (Tokyo)* **62**, 55–61 (2009).
- 10 Zhang, C. *et al.* Isolation, structure and antibacterial activity of pleosporone from a pleosporalean ascomycete discovered by using antisense strategy. *Bioorg. Med. Chem.* **17**, 2162–2166 (2009).
- 11 Wang, J. *et al.* Platensimycin is a selective FabF inhibitor with potent antibiotic properties. *Nature* **441**, 358–361 (2006).
- 12 Singh, S. B. *et al.* Isolation, structure, and absolute stereochemistry of platensimycin, a broad spectrum antibiotic discovered using an antisense differential sensitivity strategy. *J. Am. Chem. Soc.* **128**, 11916–11920 and 15547 (2006).
- 13 Wang, J. *et al.* Platencin is a dual FabF and FabH inhibitor with potent in vivo antibiotic properties. *Proc. Natl Acad. Sci. USA* **104**, 7612–7616 (2007).
- 14 Jayasuriya, H. *et al.* Isolation and structure of platencin: a novel FabH and FabF dual inhibitor with potent broad spectrum antibiotic activity produced by *Streptomyces platensis* MA7339. *Angew. Chem. Int. Ed.* **46**, 4684–4688 (2007).
- 15 Young, K. *et al.* Discovery of FabH/FabF inhibitors from natural products. *Antimicrob. Agents Chemother.* **50**, 519–526 (2006).
- 16 Ondeyka, J. G. *et al.* Discovery of bacterial fatty acid synthase inhibitors from a phoma species as antimicrobial agents using a new antisense based strategy. *J. Nat. Prod.* **69**, 377–380 (2006).
- 17 Kodali, S. *et al.* Determination of selectivity and efficacy of fatty acid synthesis inhibitors. *J. Biol. Chem.* **280**, 1669–1677 (2005).
- 18 Donald, R. G. *et al.* A *Staphylococcus aureus* fitness test platform for mechanism-based profiling of antibacterial compounds. *Chem. Biol.* **16**, 826–836 (2009).
- 19 Huber, J. *et al.* Chemical genetic identification of peptidoglycan inhibitors potentiating carbapenem activity against methicillin-resistant *Staphylococcus aureus*. *Chem. Biol.* **16**, 837–848 (2009).
- 20 Jiang, B. *et al.* Pap inhibitor with in vivo efficacy identified by *Candida albicans* genetic profiling of natural products. *Chem. Biol.* **15**, 363–374 (2008).
- 21 Parish, C. A. *et al.* Isolation and structure elucidation of parnafungins, antifungal natural products that inhibit mRNA polyadenylation. *J. Am. Chem. Soc.* **130**, 7060–7066 (2008).
- 22 Herath, K. *et al.* Isolation, structure and biological activity of phomafungin, a cyclic lipopeptide from a widespread tropical *Phoma* sp. *Bioorg. Med. Chem.* **17**, 1361–1369 (2009).
- 23 Ondeyka, J. *et al.* Isolation, structure elucidation, and biological activity of virgineone from *Lachnum virgineum* using the genome-wide *Candida albicans* fitness test. *J. Nat. Prod.* **72**, 136–141 (2009).
- 24 Xu, D. *et al.* Genome-wide fitness test and mechanism-of-action studies of inhibitory compounds in *Candida albicans*. *PLoS Pathog.* **3**, e92 (2007).
- 25 Hensens, O. D. *et al.* Isolation and structure of flutimide, a novel endonuclease inhibitor of influenza virus. *Tetrahedron Lett.* **36**, 2005–2008 (1995).
- 26 Singh, S. B. & Tomassini, J. E. Synthesis of natural flutimide and analogous fully substituted pyrazine-2,6-diones, endonuclease inhibitors of influenza virus. *J. Org. Chem.* **66**, 5504–5516 (2001).
- 27 Singh, S. B. Total synthesis of flutimide, a novel endonuclease inhibitor of influenza virus. *Tetrahedron Lett.* **36**, 2009–2012 (1995).
- 28 Savard, M. E., Melzer, M. S., Boland, G. J., Bensimon, C. & Blackwell, B. A. A new 1-hydroxy-2,6-pyrazinedione associated with hypovirulent isolates of sclerotinia minor. *J. Nat. Prod.* **66**, 306–309 (2003).
- 29 Chinworrungsee, M., Kittakoop, P., Saenboonrueng, J., Kongsaree, P. & Thebtaranonth, Y. Bioactive compounds from the seed fungus *Menisporopsis theobromae* BCC 3975. *J. Nat. Prod.* **69**, 1404–1410 (2006).
- 30 Sheldrick, G. M. Phase annealing in SHELX-90: direct methods for larger structures. *Acta Crystallogr.* **A46**, 467–473 (1990).
- 31 Sheldrick, G. M. A Short History of SHELX. *Acta Crystallogr.* **A64**, 112–122 (2008).
- 32 Onishi, H. R. *et al.* Antibacterial agents that inhibit lipid A biosynthesis. *Science* **274**, 980–982 (1996).
- 33 Wang, J. *et al.* Discovery of a small molecule that inhibits cell division by blocking FtsZ, a novel therapeutic target of antibiotics. *J. Biol. Chem.* **278**, 44424–44428 (2003).
- 34 Singh, S. B. *et al.* Antibacterial evaluations of thiazomycin- a potent thiazolyl peptide antibiotic from *Amycolatopsis fastidiosa*. *J. Antibiot. (Tokyo)* **60**, 565–571 (2007).